

# We are IntechOpen, the world's leading publisher of Open Access books Built by scientists, for scientists

6,900

Open access books available

186,000

International authors and editors

200M

Downloads

Our authors are among the

154

Countries delivered to

TOP 1%

most cited scientists

12.2%

Contributors from top 500 universities



WEB OF SCIENCE™

Selection of our books indexed in the Book Citation Index  
in Web of Science™ Core Collection (BKCI)

Interested in publishing with us?  
Contact [book.department@intechopen.com](mailto:book.department@intechopen.com)

Numbers displayed above are based on latest data collected.  
For more information visit [www.intechopen.com](http://www.intechopen.com)



---

# Diverse Thermal Transport Properties of Two-Dimensional Materials: A Comparative Review

---

Guangzhao Qin and Ming Hu

Additional information is available at the end of the chapter

<http://dx.doi.org/10.5772/64298>

---

## Abstract

The discovery of graphene led to an upsurge in exploring two-dimensional (2D) materials, such as silicene, germanene, phosphorene, hexagonal boron nitride (*h*-BN), and transition metal dichalcogenides (TMDCs), which have attracted tremendous attention due to their unique dimension-dependent properties in the applications of nanoelectronics, optoelectronics, and thermoelectrics. The phonon transport properties governing the heat energy transfer have become a crucial issue for continuing progress in the electronic industry. This chapter reviews the state-of-the-art theoretical and experimental investigations of phonon transport properties of broad 2D nanostructures in various forms, with graphene, silicene and phosphorene as representatives, all of which consist of single element. Special attention is given to the effect of different physical factors, such as sample size, strain, and layer thickness. The effect of substrate and the phonon transport properties in heterostructures are also discussed. We find that the phonon transport properties of 2D materials largely depend on their atomic structure and interatomic bonding nature, showing a diverse intrinsic phonon behavior and disparate response to external environment.

**Keywords:** two-dimensional materials, thermal conductivity, phonon transport, strain, substrate, first-principles

---

## 1. Introduction

Graphene, a two-dimensional (2D) atomic thin honeycomb lattice, exhibits numerous striking physical properties, and can, in principle, be considered as an elementary building block for all carbon allotropes. Ever since the recent developments in 2004, the field of graphene research took off rapidly. These developments in the science of graphene prompted an unprecedented

surge of activity and demonstration of new physical phenomena. Despite its success, graphene still faces some severe problems in its nature of semi-metal or zero band-gap semiconductor and its incompatibility with the current Si-based semiconductor technology. Given that the honeycomb geometry is related to some of the exceptional properties of graphene, there is strong motivation to investigate whether changing carbon to other atom type might give rise to novel physical phenomena as well. An intuitive idea is to study similar 2D materials, such as silicene and phosphorene. Actually, silicene, the Si counterpart of graphene, can solve the above-mentioned problems smoothly and thus has received intense interest lately. Given the fact that thermal transport plays a critical role in many applications such as heat dissipation in nanoelectronics and thermoelectric energy conversion, there has been an emerging demand in characterizing thermal (mainly phonons) transport property of silicene structures. Moreover, research results have shown that silicene exhibits a few novel thermal transport properties, which are fundamentally different from that of graphene, despite the similarity of their honeycomb lattice structure. Therefore, the abnormal physical property, primarily stemming from its unique low buckling structure, may enable silicene to open up entirely new possibilities for revolutionary electronic devices and energy conversion materials.

With the state of the art, this book chapter aims to present theoretical investigations of thermal transport of broad 2D nanostructures in various forms, which have been carried out in our research group in the past few years. Heat transfer in such structures is not only directly relevant to optimizing the device performance such as improved thermal management for nanoelectronics and thermoelectric energy conversion efficiency, but also is a scientifically fundamental problem for many other similar two-dimensional systems (**Figure 1**).

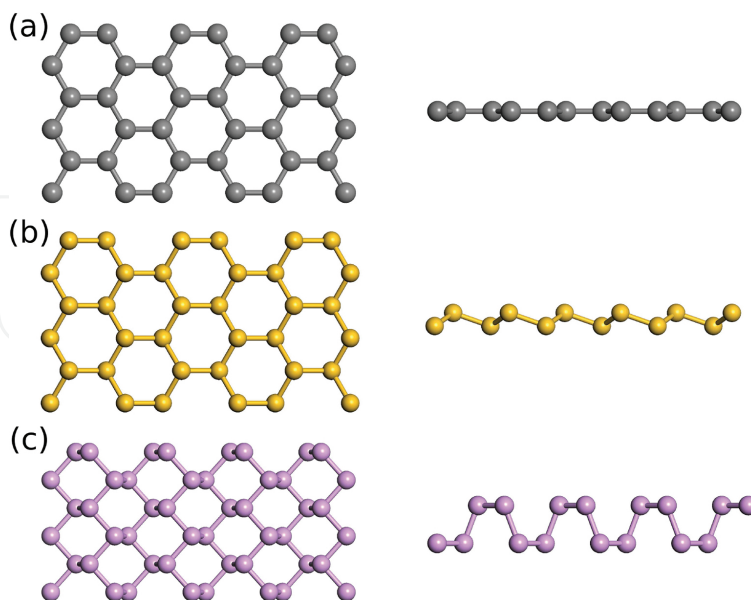


**Figure 1.** Comparison of the crystal structures (top view and side view) among (a) graphene, (b) silicene, and (c) phosphorene. Graphene possesses perfect planar structure, silicene possesses low buckling structure, and phosphorene possesses pucker (hinge-like) structure.

## 2. Thermal conductivity

Two-dimensional (2D) materials have been extensively studied in the past decade because of their novel physical and chemical properties [1, 2] and potential applications [3, 4]. For example, it has been found that graphene has extremely high thermal conductivity [5], which has great potential in the applications including electronic cooling and composite materials. In this section, we summarize the available experimental data and theoretical calculations on the phonon transport properties of several typical 2D materials consisting of only one type of element, including graphene, silicene, and phosphorene (**Figure 2**).

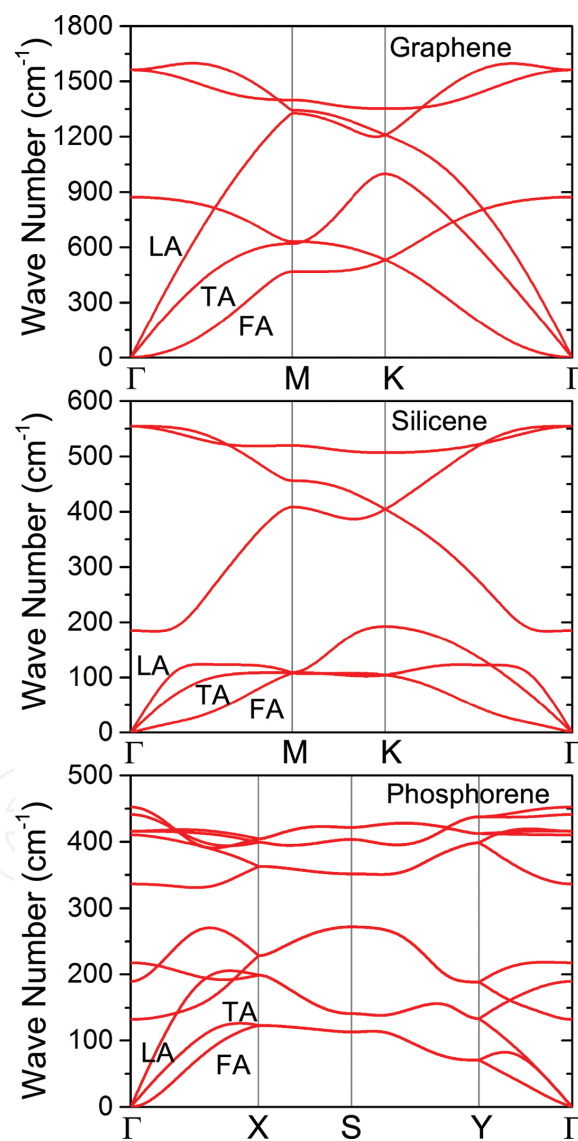


**Figure 2.** The phonon dispersion curves along the path passing through the main high-symmetry  $k$ -points in the irreducible Brillouin zone of graphene, silicene, and phosphorene. Three acoustic phonon modes (LA, TA, and FA) are labeled.

## 2.1. Graphene

Graphene, the first two-dimensional atomic crystal available to us, has attracted great attention due to its supreme mechanical, electronic, and optical properties. Besides these properties, thermal and thermoelectric properties of graphene are also very fascinating. Experiments have shown that the thermal conductivity of graphene reaches as high as about 3000 W/mK, which makes graphene very promising for thermal management applications such as heat dissipation in electronics [5]. In addition to the heat dissipation applications, due to its extremely high electrical conductivity, graphene has also been explored to be used as thermoelectric material by largely reducing its thermal conductivity by varieties of functionalization, such as constructing graphene nanoribbons, hydrogenation, defects, and doping.

There have been a long time for an intriguing open question on the phonon transport in graphene: what is the relative contribution to heat conduction of LA, TA, and FA phonon polarization branches? The focused point is the importance of FA phonons from negligible to dominant. Klemens' theory states that thermal energy is mainly carried by longitudinal acoustic (LA) and transverse acoustic (TA) phonons, and contributions from out-of-plane flexural acoustic (FA) phonons are negligible due to their small group velocity in the Brillouin zone center and large Grüneisen parameter [6–8]. However, based on recent studies, the arguments for the dominant contributions of FA modes are made on the basis of the symmetry-based phonon-phonon scattering selection rule [9–11]. As for graphene, because of the reflectional symmetry of the structure, the phonon scattering processes involving odd number of FA modes are not allowed, which restricts the phase space for phonon-phonon scattering [9]. The suppression of scattering of FA leads to its extremely low scattering rate which is equivalent to a very large phonon lifetime, which results in the huge contribution to thermal conductivity from FA modes. The selection rule can be broken by placing graphene on any substrate or due to the presence of nanoscale corrugations. Therefore, it is intuitive to see that thermal conductivity of supported graphene is dramatically reduced.

## 2.2. Silicene

Silicene, the silicon counterpart of graphene, possesses a two-dimensional structure that leads to a host of interesting physical and chemical properties of significant utility. Compared to graphene, silicene is more compatible with silicon-based semiconductor devices and technologies, and therefore has greater potential in nanoelectronic applications. In particular, in terms of thermoelectric application, silicene is even more exciting than graphene as the charge carrier of silicene is massless fermion, and the electrical conductivity of silicene is as high as that of graphene. At the same time, the thermal conductivity of silicene is expected to be much lower than that of graphene due to its buckled atomic structure. In addition to thermoelectric applications, silicene, with supreme electronic properties similar to those of graphene, has also shown great potential for other applications, such as nanoelectronics. For example, in contrast to graphene, the buckled atomic structure breaks the symmetry of the silicene, making it possible to open a band gap by applying electric field [12–14]. Monolayer silicene has been successfully fabricated on substrates such as Ag(1 1 0) [15], Ir(1 1 1) [16], and Ag(1 1 1) [17] surfaces. Recently, Tao et al. have demonstrated silicene-based transistors can operate at room

temperature [4]. Although the performance is still moderate and the lifetime of this transistor is only a few minutes, it has attracted significant research interest in silicene-based devices [18–20]. Therefore, there is an urgent demand to quantify the thermal transport property of silicene, and it is of great interest to explore the role of buckled lattice on phonon transport mechanisms compared with the planar graphene.

The intrinsic physical properties of silicene, such as lattice thermal conductivity, have been an active area of research. Although the thermal conductivity of silicene has not been measured in experiments due to the difficulty of synthesizing freestanding silicene, several numerical simulations have predicted the thermal conductivity of silicene and the results at 300 K range from 5 to 69 W/mK [21–23]. Most of the numerical simulations are based on classical molecular dynamics and the discrepancy of results mainly arises from the different interatomic interaction potentials used. Notably, first-principles-based lattice dynamics predicted that the thermal conductivity of silicene is in the range of 20–30 W/mK [23, 24], which should be more reliable.

From the aspect of theoretical study, the widely used classical molecular dynamics simulation is an appropriate way to investigate the transport phenomena and mechanisms in silicene. Based on the optimized SW potential of SW1 and SW2 obtained by Zhang et al. [21], the thermal conductivity of silicene calculated from non-equilibrium molecular dynamics (NEMD) is 8.64 W/mK (SW1) and 11.77 W/mK (SW2) at 230 K. One would notice that the results for the equilibrium molecular dynamics (EMD) and NEMD methods are not the same, even after the thermal conductivity was extrapolated to infinitely long in the case of NEMD simulation. Nevertheless, the results confirm that the thermal conductivity of monolayer silicene is ultra-low, which is one order of magnitude lower than the value of bulk silicon (about 150 W/mK from experiments).

The thermal conductivity was also calculated by Xie et al. using the single-mode relaxation time (SMRT) model derived from Boltzmann transport equation (BTE), where the scattering of certain phonon mode is irrelevant to the condition of other phonon modes, but other phonon modes are assumed to stay in their equilibrium condition. The interactions for silicon atoms are described by the SW1/SW2 potentials, and the single-point energies are calculated using the Large-scale Atomic/Molecular Massively Parallel Simulator (LAMMPS) package. The thermal conductivity values at 300 K are 3.33 W/mK for the optimized SW1 parameters and 5.43 W/mK for the optimized SW2 parameters. The thermal conductivity calculated by anharmonic lattice dynamics (ALD) is smaller than that calculated by molecular dynamics (MD) simulations. The discrepancy was argued to be mainly attributed to the strong normal scattering near the zone center in two-dimensional materials, as also seen in graphene. After that, first-principles-based ALD method is combined with BTE to accurately calculate the lattice thermal conductivity of silicene by Xie et al. [24]. The main difference from the previous study is that the interactions among atoms are described based on first-principles calculations, and the accuracy should be much higher. The temperature dependence of thermal conductivity was explicitly considered and mode-specific contribution to overall thermal conductivity was analyzed and discussed. Due to the buckling structure of silicene, the flexural mode is not purely out-of-plane vibration, but also contains small components in the in-plane directions.



The intrinsic lattice thermal conductivity of silicene is 9.4 W/mK at 300 K. Later on, due to the development of the calculation method, the BTE can be iteratively solved, where the thermal conductivity becomes unbounded and the iterative procedure reflects the process of the redistribution of phonon modes driven by the heat flux [11, 25–27]. However, the underlying mechanisms are still not well understood. Based on the iterative solution of BTE, the thermal conductivity of silicene is in the range of 15–30 W/mK for three finite sizes of 0.3, 3, and 30  $\mu\text{m}$  [28]. Gu and Yang and Kuang et al. also calculated the thermal conductivity of silicene using the first-principles-based BTE approach, and obtained similar magnitude of thermal conductivity [23, 29].

### 2.3. Phosphorene

Black phosphorus (BP) is another emerging material which has a puckered layered structure with intra-layer interaction dominated by van der Waals forces [30–32]. Few-layer BP has recently been successfully fabricated by mechanical exfoliation [33, 34] and has generated tremendous interest among scientists [33–44]. Phosphorene, the single layer counterpart of BP, is another interesting 2D structure with high carrier mobility proved by experiments [33, 34, 36] and a large fundamental direct band gap ( $\sim 1.5$  eV) [39], which makes BP promising for lots of nanoelectronic applications [32]. For example, some previous theoretical and experimental works have illustrated that phosphorene can be used as nanoelectronic devices, such as field-effect transistors and photo-transistors [33, 34, 36–38]. Besides the extensive studies on its electrical properties, there are also a lot of explorations on its potential applications in thermoelectrics [35, 42, 43]. All these electrical and thermoelectrical applications are closely related to thermal properties. Considering the potential valuable applications of phosphorene as nano-/opto-electronic and thermoelectric devices, it is necessary to fundamentally study the phonon transport properties of this new 2D material.

There have been some experiment works on the measurement of the thermal conductivity of bulk BP [45] and phosphorene films with different thicknesses [46–48]. The thermal conductivity of monolayer phosphorene was also reported theoretically by several independent groups using various methods, such as analytical estimations [35, 49], MD simulation with optimized Stillinger-Weber potential [50–52], relaxation time approximation (RTA) [45, 53–55], and iterative method for solving BTE [45, 54]. However, the exact value of the lattice thermal conductivity of monolayer phosphorene is still unclear, since these results are even one order of magnitude different from each other. For example, the thermal conductivity of monolayer phosphorene along zigzag direction ranges from 30  $\text{W m}^{-1} \text{K}^{-1}$  to 152.7  $\text{W m}^{-1} \text{K}^{-1}$ , while that along armchair direction ranges from 9.9  $\text{W m}^{-1} \text{K}^{-1}$  to 63.9  $\text{W m}^{-1} \text{K}^{-1}$  [35, 50–52]. The huge deviation might be due to the different calculation methods or parameters. For example, Jain et al. calculated the thermal conductivity using similar iterative method based on ALD/BTE as employed in this work, and the test for the convergence of thermal conductivity was performed with respect to the interactions cutoff [54]. However, the thermal conductivity does not show a distinct convergence trend versus the interactions cutoff while jumps in a quite wide range, which might lie in that: (1) the lacking of long-range electrostatic interactions in their work, which are taken into account by adding to the dynamical matrix a correction

from dielectric tensor and Born effective charges; (2) the scalar relativistic pseudopotential used in their work does not involve the van der Waals interactions, which are considered having significant effect on the properties of bulk BP and phosphorene [31, 56]. In another work by Zhu et al. [53] based on RTA, the interactions range of third-order Interatomic force constants (IFCs) is truncated up to 4.4 Å, with which the interaction is only taken into account up to 7th nearest neighbors. Therefore, to end the confusing situation, it is necessary to perform systematic study to precisely quantify the phonon transport properties of phosphorene, which would be of significance to its further applications in nano-/opto-electronics and thermoelectrics (Figure 3).

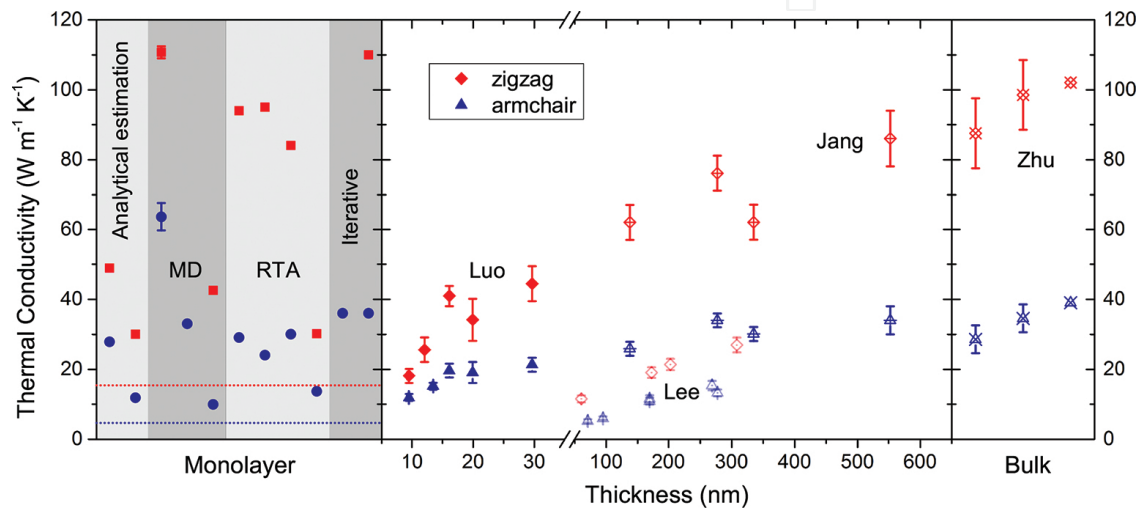


**Figure 3.** The comparison of the thermal conductivity obtained from experiments and theoretically reported results. The left box shows the thermal conductivity of monolayer phosphorene from different methods [35, 45, 49–55]. The middle box shows the thermal conductivity of phosphorene films with different thicknesses from experiments [46–48]. The right box shows the thermal conductivity of bulk BP from both experiment and theoretical calculation [45].

The thermal conductivity of monolayer phosphorene is in the same order of magnitude as that of silicene ( $\sim 20 \text{ W m}^{-1} \text{ K}^{-1}$ ) [21–24, 28], while two orders of magnitude lower than that of graphene ( $3000\text{--}5000 \text{ W m}^{-1} \text{ K}^{-1}$ ) [9, 11]. The thermal conductivity is mainly contributed by phonon modes below the gap which separates the phonon branches into two regions with each region containing six branches. The phonon modes in the region below the gap contribute more than 85% to the thermal conductivity, and dominate the anisotropy. The thermal conductivity along armchair direction is mainly contributed by LA, while along zigzag direction, TA/FA also contribute a lot to the thermal conductivity besides LA. The contributions to thermal conductivity along zigzag and armchair directions from FA are 16% and 8% at room temperature, respectively, which is close to that of silicene (7.5%) but much smaller than that of graphene (75%) [11, 23]. As for graphene, because of the reflectional symmetry of the structure, the phonon scattering processes involving odd number of FA modes are not allowed, which is the so-called symmetry-based phonon-phonon scattering selection rule [9]. Compared with graphene, the symmetry-based phonon-phonon scattering selection rule is broken by the hinge-like structure of phosphorene, resulting in a large scattering rate of FA,



which thus leads to its small contribution to the thermal conductivity. Note that FA contributes to the thermal conductivity along zigzag direction more than that along armchair direction. The reason might lie in the feature of the hinge-like structure that it is more “uneven” along armchair direction because of the up and down of the sublayers chains.

### 3. Effect of different physical factors

#### 3.1. Length dependence

As for the length dependence of the thermal conductivity of silicene, regarding the convergence with respect to the  $q$  mesh, it seems that for infinite size (without boundary scattering), the thermal conductivity tends to diverge with denser  $q$  mesh, while for finite size the thermal conductivity converges. The possible divergence of thermal conductivity for 2D materials has raised a lot of debate recently. For example, in [23] it was claimed that the thermal conductivity of silicene would diverge with the sample size. Similar conclusions have been drawn in some other literature for graphene [57]. However, there have been strong debates on the possible divergence of thermal conductivity of graphene. On the other hand, Fugallo et al. argue that the thermal conductivity of graphene converges when the simulated sampling size goes up to 1 mm [58]. In their work, exact phonon BTE is solved and first-principles calculations are employed to extract harmonic and anharmonic IFCs. Barbarino et al. also reach the same conclusion with approach-to-equilibrium molecular dynamics simulations for graphene sample of 0.1 mm in size [59]. By using a finite  $q$  mesh, the extremely long wavelength acoustic phonon modes are actually excluded, which are believed to be responsible for the possible divergence of the thermal conductivity [57]. For finite sample size, the boundary scattering imposes a limit on the phonon mean free path (MFP) to avoid divergence. For real applications, a finite sample has to be used, and the wrinkles and defects are generally unavoidable, so the sample cannot have diverged thermal conductivity.

As for monolayer phosphorene, Zhu et al. claimed that there exists a compelling coexistence of size-dependent and size-independent thermal conductivities along zigzag and armchair directions, respectively [53], which is distinctly different from isotropic and divergent thermal conductivities in two-dimensional graphene and silicene. The size-dependent thermal conductivity is due to the lifetime of acoustic phonon modes quickly blowing up approaching the  $\Gamma$  point of the Brillouin zone [57]. The contributions of FA, TA, LA, and optical phonon modes to the total thermal conductivity are plotted to further understand the dependence of  $\kappa_{zz}$  on the size of the  $q$  mesh. It is found that the thermal conductivities contributed by FA, LA, and all optical phonons do not change with the increasing size of the  $q$  mesh. The divergent  $\kappa_{zz}$  is mainly due to the contribution from TA branch.

#### 3.2. Strain

Despite recent efforts to describe the properties of unstrained materials, in real applications, nanoscale devices usually contain residual strain after fabrication [60]. It is thus important to

investigate possible strain effects on the properties of materials, especially phonon transport properties.

As for graphene, the application of tensile strain will give three noticeable changes that can affect  $\kappa$ : (1) lowered TO and LO phonon branches; (2) linearized zone-center ZA phonon branch; (3) weakened anharmonic IFCs [11]. Full solution of the BTE gives  $\kappa$  relatively strain independent up to 1% isotropic strain, which is a balanced result of the following aspects. With the increase of tensile strain, the ZA branch near the zone center becomes linear with increasing slope, leading to the increase of near zone center ZA phonon velocities and the decrease of density of ZA phonons. The character of the acoustic phonon-phonon scattering also changes due to these changes of the phonon dispersion. In addition, the tensile strain weakens the anharmonic IFCs, which acts to increase  $\kappa$ , but this is balanced by the changes in the phonon dispersion that tend to decrease  $\kappa$ . Furthermore, the lowered TO and LO branches play only a minor role in reducing  $\kappa$  through increased *acoustic + acoustic*  $\leftrightarrow$  *optic* three-phonon scattering.

It was found that a mechanical tensile strain less than 5% could tune the electronic structure of silicene [61] and larger tensile strain (7.5%) could induce a semimetal-metal transition [62]. On the other hand, using first-principles it has been demonstrated that the silicene structure remains buckled even when 12.5% tensile strain is applied [62, 63]. In comparison to the structural and electronic properties, the strain effect on the lattice thermal conductivity of silicene is also investigated. Pei et al. [64] and Hu et al. [22] investigated the effect of uniaxial strain on the thermal conductivity based on the classical NEMD method. Pei et al. studied tensile strain up to 12% and concluded that the thermal conductivity first increases slightly (around 10% increment) and then decreases with an increased amount of tensile strain. Hu et al. found that the thermal conductivity of silicene sheet and silicene nanoribbon experiences monotonic increase by a factor of two with tensile strain up to 18%. The modified embedded-atom method (MEAM) [65] and original Tersoff potential [66] were used in their simulations, respectively. However, both potentials are developed for bulk silicon, thus directly applying those potentials to the new 2D silicene structure is questionable. For example, the Tersoff potential cannot even reproduce the buckled structure of silicene and the MEAM potential seems to overestimate the buckling distance. It is well known that the interatomic potential directly determines the quality of classical molecular dynamics simulation. Therefore, in order to precisely predict the strain effect on the lattice thermal conductivity of silicene and identify the underlying mechanism, it is necessary to calculate the lattice thermal conductivity of silicene under different strains using a more accurate method.

The strain-dependent thermal conductivity of monolayer silicene was recently studied based on single mode RTA and iterative solution of the BTE by Xie et al. [28], where the harmonic and anharmonic force constants are determined using first-principles calculations. Both methods yield a similar trend in the change of thermal conductivity with respect to tensile strain. It is shown that within 10% tensile strain, the thermal conductivity of silicene first increases dramatically and then decreases slightly. The maximum thermal conductivity was found when 4% tensile strain was applied, and the value was about 7.5 times that of the unstrained case. Such a dramatic change is quite unusual for solid materials, and could be used

as a thermal switch together with thermal diodes to build thermal circuits. This trend is mainly due to the strain-dependent phonon lifetime, which is related to the variations of both harmonic and anharmonic force constants under strain. FA phonon lifetimes increase significantly under tensile strain because the structure becomes more planar, which leads to a large increase of their contribution to overall thermal conductivity, but is not the major reason for the significant change of overall thermal conductivity within 4% strain. The significant enhancement of thermal conductivity from 0 to 4% strain is mainly due to the reduced scattering of TA and LA phonons with FA phonons. The result suggests that other 2D materials with intrinsic buckling may have similar strain dependence of thermal conductivity, which is left for further investigation. Almost at the same time, Kuang et al. used a similar method to study the phonon transport properties of silicene with strain applied, and obtained similar results [29]. They also found a strong size dependence of  $\kappa$  for silicene with tensile strain, i.e., divergent  $\kappa$  with increasing system size. However, based on their calculations, the intrinsic room temperature  $\kappa$  for unstrained silicene converges with system size to 19.34 W/mK at 178 nm. They analyzed that the convergence behavior of thermal conductivity may be significantly affected by the out-of-plane acoustic phonon branch. The divergence of thermal conductivity with respect to system size is resulted from the linear behavior of FA at low frequencies, which is very different from the familiar quadratic nature for the corresponding branch in unstrained graphene. The origin of the size effect stems from nonzero contributions of FA modes at the long wavelength limit. Although physically this still demands further careful investigation, technologically speaking, using a larger supercell for the calculations of harmonic IFCs and the phonon dispersion should effectively suppress the divergence of thermal conductivity with respect to system size.

As for phosphorene, the strain effect on the thermal conductance was studied by Ong et al. using the first-principles-based non-equilibrium Green's function (NEGF) method, which yields the thermal transport behavior in the ballistic limit [67]. They find that the thermal conductance anisotropy with the orientation can be tuned by applying strain. In particular, the thermal conductance of phosphorene in zigzag direction is found to be enhanced when the strain is applied, but decreases when the strain is applied in the armchair direction; whereas the thermal conductance in armchair direction always decreases regardless of the strain direction.

Besides, Zhang et al. performed NEMD simulations to study the strain effect on the thermal conductivity of phosphorene [52]. The results show a clear trend that the thermal conductivity increases with the tensile strain and decreases with the compressive strain, which can be explained from the buckling deformation and is consistent with that of graphene. Moreover, the thermal conductivity along the zigzag direction increases slightly when the tensile strain is 0.01, and thereafter reaches a plateau until the strain level of 0.04, which may be attributed to the tension-induced elongation of the phosphorene sample.

### 3.3. Thickness dependence

For the thermal conductivity of few-layer films, there are two aspects affecting the phonon transport: (1) intrinsic properties of few layers, that is, crystal anharmonicity; (2) extrinsic

effects such as phonon-boundary or defect scattering. The optothermal Raman study found that  $\kappa$  of suspended uncapped few-layer graphene decreases with increasing number of layers, approaching the bulk graphite limit, which was explained by considering the intrinsic quasi-2D crystal properties described by the phonon Umklapp scattering. As the thickness increases, the phonon dispersion changes and more phase-space states become available for phonon scattering, resulting in the decrease of thermal conductivity. The small thickness ( $< 4$ ) also means that phonons do not have a transverse component of group velocity, leading to weak phonon scattering from the top and bottom boundaries, especially if constant  $n$  is maintained over the whole area of the flake. The boundary scattering will increase if  $n > 4$ , because the transverse component of the group velocity is not equal to zero, and it is harder to maintain constant  $n$  through the whole area of an FLG flake, resulting in  $\kappa$  below the graphite limit. The graphite value recovers for thicker films.

The layer effect on the thermal conductivity of phosphorene was studied by Zhang et al. based on NEMD simulations [52]. It was found that the thermal conductivities along the two in-plane directions are insensitive to the number of layers, which is in sharp contrast to that of graphene, as it was shown that the thermal conductivity in multi-layer graphene decreases with increasing layer number. The underlying physical origin of the layer-independent thermal conductivity of multi-layer phosphorene was explained that unlike graphene with only one-atom thickness, the atoms in single-layer phosphorene are arranged in two sub-layers and formed a puckered geometry, which hinders the out-of-plane (flexural) phonon mode and thus diminishes the layer effect in multi-layer phosphorene. It is worth pointing out that the Lennard-Jones (LJ) potential is used for the van der Waals (vdW) interactions across different layers in multi-layer phosphorene in their work. Based on the studies of Qiao et al. and Hu et al. [31, 56], as confirmed with the real-space wave functions, the coupling between layers in few-layer black phosphorus is mediated by interactions that are much stronger than van der Waals (vdW) as in graphene or TMDCs. Considering the significant effect of interlayer interactions on the thermal conductivity, the use of vdW to quantify the interactions in the MD is questionable. Further works based on accurate first-principles calculations are needed to address the layer-dependent thermal conductivity of few-layers black phosphorus (phosphorene) in detail, which is ongoing in our group currently.

### 3.4. Effect of substrate

Supported silicene is, in fact, a common form in realistic applications. For example, it can be transferred onto an insulating substrate and gated electrically. The effects of different substrates on the thermal transport of silicene were studied by Zhang et al. recently based on NEMD simulations using the optimized SW potential for silicene [68]. They observe that the thermal conductivity of silicene can be bilaterally changed with different surface crystal plane of the substrate. The phenomenon found here is fundamentally different from our general understanding of monolayer graphene supported on substrate, where the substrate always has a negative effect on the in-plane thermal transport. The discrepancy between monolayer graphene and silicene can be explained in terms of different effects induced by the substrate on the phonon transport, specifically, the competition between the out-of-plane flexural modes



and the in-plane modes. This mechanism is further linked to the different atomic structure, i.e., for graphene, it is planar (no buckling distance), while silicene has a buckling distance of about 0.42 Å. By performing phonon polarization and spectral energy density (SED) analysis, the authors further revealed the underlying physics of the novel phenomenon in terms of the different impacts on the dominant phonons in the thermal transport of silicene induced by the substrate. These results indicate that by choosing different substrates, the thermal conductivity of 2D silicene can be largely tuned, which paves the way for manipulating the thermal transport properties of silicene for future emerging applications.

Very recently, the thermal conductivity of silicene supported in an amorphous silicon dioxide ( $\text{SiO}_2$ ) for temperature ranging from 300 to 900 K was studied by Wang et al. from MD simulations [69]. They found that the thermal conductivity of silicene has a substantial reduction with increasing temperature, and putting silicene on amorphous  $\text{SiO}_2$  leads to 78% reduction in the overall thermal conductivity of silicene at room temperature. They further compared model-level phonon properties, such as phonon relaxation times and phonon mean free paths (MFPs) of freestanding and supported silicene at 300 K. It is found that the phonon relaxation time in the case of supported silicene is reduced from 1–13 ps to 1 ps, and corresponding MFPs decrease from 10–120 nm to 0–20 nm. The thermal conductivities of free-standing and supported silicene are mainly (more than 85%) contributed by the longitudinal and transverse acoustic phonons, while the out-of-plane acoustic phonons have a negligible contribution of less than 3%. These results are in line with those found previously [68].

#### 4. Heterostructures

In electronics, especially for nanoelectronics, interfacial thermal resistance is a key factor that affects heat dissipation in devices and researchers have shown that the interfacial thermal transport can be largely enhanced using graphene-based nanocomposites as thermal interface materials. Graphene and its bilayer structure are the two-dimensional crystalline forms of carbon, whose extraordinary electron mobility and other unique features hold great promise for nanoscale electronics and photonics. Their realistic applications in emerging nanoelectronics usually call for thermal transport manipulation in a controllable and precise manner. Equilibrium molecular dynamics simulations were performed by Zhang et al. to investigate the effect of interlayer  $sp^3$  bonding density on the thermal conductivity of bilayer graphene, especially the results of the randomly and regularly bonded bilayer graphene structures were compared in detail [70]. The thermal conductivity of randomly bonded bilayer graphene decreases monotonically with the increase of interlayer bonding density, which follows the same trend as that obtained in the literature. However, for the regularly bonded bilayer graphene structure, They observed the unexpected non-monotonic interlayer bonding density dependence of thermal conductivity. The phonon spectral energy density, participation ratio, and mode weight factor analyses were performed to explore the underlying mechanism of this counterintuitive phenomenon. It is found that the lifetimes of low-frequency (<5 THz) phonons for randomly and regularly bonded bilayer graphene are nearly the same, which is consistent with the general knowledge that the low-frequency phonons are not sensitive to the detailed



interfacial bonding configuration, considering that the characteristic size of the covalent bonding is in the order of only a few angstroms, which is much shorter than the typical wavelength of the low frequency phonons. In contrast, for medium-frequency (5–30 THz) and high-frequency (30–50 THz) phonons, the lifetimes in the regularly bonded bilayer graphene are quite larger than that of randomly bonded structure, especially for the medium-frequency phonon modes which have a rather large contribution to the higher thermal conductivity of the regularly bonded bilayer graphene than the randomly bonded structure. By evaluating the relative importance of the contributions of phonon lifetime and square of phonon group velocity, we conclude that compared with random bonding, the much higher thermal conductivity of the regularly bonded bilayer graphene is mainly due to the large enhancement in the group velocity of the phonon modes in the medium-frequency range (5–30 THz). In addition, the thermal conductivity of bilayer graphene depends not only on the interlayer bonding density, but also the detailed topological arrangement of the interlayer  $sp^3$  bonds. Comparing the regularly bonded bilayer graphene between different bonding densities, the change of phonon lifetime, instead of the change of group velocity, is the main reason for the non-monotonic thermal conductivity dependence. The phonon mode localization is characterized by calculating the participation ratio and provides evidence that the participation ratio at different bonding density resembles the non-monotonic dependent thermal conductivity. Again this can be correlated with their atomic structure, where the regular bonding density of 6.25% and 12.5% has more homogeneous  $sp^3$  bonding than that of other bonding densities, which should be responsible for their different phonon band structure.

## 5. Concluding remarks and perspectives

The present chapter has surveyed the recent advancements in understanding the phonon transport properties of some representative two-dimensional materials, which are one of the fastest growing emerging fields in nanostructured semiconductors and nanocrystals. The thriving expansion of new capabilities of two-dimensional semiconductors has progressed rapidly during the last few years. While physical fundamentals for electronic properties of this class of nanomaterials have been well understood and explored extensively, limited understanding has been achieved in thermal transport properties. Although most of two-dimensional materials have as simple as honeycomb lattice structure, revealing the phonon transport mechanism in such atomic thin materials seems not an easy task. Phonon transport in graphene is the first success in this line. However, the previous understanding achieved for graphene cannot be straightforwardly extended to other similar two-dimensional materials. In this chapter, we demonstrated a comparative study of the phonon transport properties between graphene, silicene, and phosphorene and found that these three materials could have fundamentally different governing mechanism in heat conduction. We also analyze the detailed mechanism from different aspects.

Despite the significant accomplishment that has been gained in understanding different behavior of phonon transport in two-dimensional materials in the last few years, some important physical fundamentals still remain to be clarified. For example, the thickness-

dependent thermal conductivity of few-layer two-dimensional structures and phonon interactions between two-dimensional monolayer and substrate demand further systematic study. In addition, the two-dimensional materials-based heterostructures could possess even more diverse and fantastic phonon transport behavior, which could open up new building blocks for the next generation of advanced functional 3D devices.

## Acknowledgements

The authors acknowledge the support by the Deutsche Forschungsgemeinschaft (DFG) (project number: HU 2269/2-1).

## Author details

Guangzhao Qin<sup>1</sup> and Ming Hu<sup>1,2\*</sup>

\*Address all correspondence to: hum@ghi.rwth-aachen.de

1 Institute of Mineral Engineering, Division of Materials Science and Engineering, Faculty of Georesources and Materials Engineering, RWTH Aachen University, Aachen, Germany

2 Aachen Institute for Advanced Study in Computational Engineering Science (AICES), RWTH Aachen University, Aachen, Germany

## References

- [1] Novoselov, K. S. et al. Electric field effect in atomically thin carbon films. *Science*, 2004;306:666–669. DOI: 10.1126/science.1102896
- [2] Seol, J. H. et al. Two-dimensional phonon transport in supported graphene. *Science*, 2010;328:213–216. DOI: 10.1126/science.1184014
- [3] Xu, X. et al. Length-dependent thermal conductivity in suspended single-layer graphene. *Nat. Commun.*, 2014;5:4689. DOI: 10.1038/ncomms4689
- [4] Tao, L. et al. Silicene field-effect transistors operating at room temperature. *Nat. Nano*, 2015;10:227–231. DOI: 10.1038/nnano.2014.325
- [5] Balandin, A. A. et al. Superior thermal conductivity of single-layer graphene. *Nano Lett.*, 2008;8:902–907. DOI: 10.1021/nl0731872
- [6] Balandin, A. A. Thermal properties of graphene and nanostructured carbon materials. *Nat. Mater.*, 2011;10:569–581. DOI: 10.1038/nmat3064

- [7] Klemens, P. G. Theory of thermal conduction in thin ceramic films. *Int. J. Thermophys.*, 2001;22:265–275. DOI: 10.1023/A:1006776107140
- [8] Klemens, P. G. Theory of the a-plane thermal conductivity of graphite. *J. Wide Bandgap Mater.*, 2000;7:332–339. DOI: 10.1106/7FP2-QBLN-TJPA-NC66
- [9] Lindsay, L., Broido, D. A. & Mingo, N. Flexural phonons and thermal transport in graphene. *Phys. Rev. B*, 2010;82:115427. DOI: 10.1103/PhysRevB.82.115427
- [10] Lindsay, L., Broido, D. A. & Mingo, N. Flexural phonons and thermal transport in multilayer graphene and graphite. *Phys. Rev. B*, 2011;83:235428. DOI: 10.1103/PhysRevB.83.235428
- [11] Lindsay, L. et al. Phonon thermal transport in strained and unstrained graphene from first principles. *Phys. Rev. B*, 2014;89:155426. DOI: 10.1103/PhysRevB.89.155426
- [12] Drummond, N. D., Zlyomi, V. & Fal'ko, V. I. Electrically tunable band gap in silicene. *Phys. Rev. B*, 2012;85:075423. DOI: 10.1103/PhysRevB.85.075423
- [13] Ni, Z. et al. Tunable bandgap in silicene and germanene. *Nano Lett.*, 2012;12:113–118. DOI: 10.1021/nl203065e
- [14] Kaloni, T. P., Cheng, Y. C. & Schwingenschlgl, U. Hole doped dirac states in silicene by biaxial tensile strain. *J. Appl. Phys.*, 2013;113:104305. DOI: 10.1063/1.4794812
- [15] Aufray, B. et al. Graphene-like silicon nanoribbons on Ag(1 1 0): a possible formation of silicene. *Appl. Phys. Lett.*, 2010;96:183102. DOI: 10.1063/1.3419932
- [16] Meng, L. et al. Buckled silicene formation on Ir(1 1 1). *Nano Lett.*, 2013;13:685–690. DOI: 10.1021/nl304347w
- [17] Lalmi, B. et al. Epitaxial growth of a silicene sheet. *Appl. Phys. Lett.*, 2010;97:223109. DOI: 10.1063/1.3524215
- [18] Nguyen, N.-T. Silicene transistors: silicon-based nanoelectronics from a single atom layer. *Micro Nanosyst.*, 2014;6:205–206. DOI: 10.2174/187640290604150302115649
- [19] Lian, C. & Ni, J. The effects of thermal and electric fields on the electronic structures of silicene. *Phys. Chem. Chem. Phys.*, 2015;17:13366. DOI: 10.1039/C5CP01557J
- [20] Schwierz, F., Pezoldt, J. & Granzner, R. Two-dimensional materials and their prospects in transistor electronics. *Nanoscale*, 2015;7:8261–8283. DOI: 10.1039/C5NR01052G
- [21] Zhang, X. et al. Thermal conductivity of silicene calculated using an optimized Stillinger-Weber potential. *Phys. Rev. B*, 2014;89:054310. DOI: 10.1103/PhysRevB.89.054310
- [22] Hu, M., Zhang, X. & Poulidakos, D. Anomalous thermal response of silicene to uniaxial stretching. *Phys. Rev. B*, 2013;87:195417. DOI: 10.1103/PhysRevB.87.195417

- [23] Gu, X. & Yang, R. First-principles prediction of phononic thermal conductivity of silicene: a comparison with graphene. *J. Appl. Phys.*, 2015;117(2):025102. DOI: 10.1063/1.4905540
- [24] Xie, H., Hu, M. & Bao, H. Thermal conductivity of silicene from first-principles. *Appl. Phys. Lett.*, 2014;104:131906. DOI: 10.1063/1.4870586
- [25] Lindsay, L. & Broido, D. A. Three-phonon phase space and lattice thermal conductivity in semiconductors. *J. Phys.: Condens. Matter*, 2008;20(16):165209. DOI: 10.1088/0953-8984/20/16/165209
- [26] Li, W. et al. Thermal conductivity of diamond nanowires from first principles. *Phys. Rev. B*, 2012;85:195436. DOI: 10.1103/PhysRevB.85.195436
- [27] Li, W., Lindsay, L., Broido, D. A., Stewart, D. A. & Mingo, N. Thermal conductivity of bulk and nanowire  $\text{mg}_2\text{sixsn}_1\text{x}$  alloys from first principles. *Phys. Rev. B*, 2012;86:174307. DOI: 10.1103/PhysRevB.86.174307
- [28] Xie, H. et al. Large tunability of lattice thermal conductivity of monolayer silicene via mechanical strain. *Phys. Rev. B*, 2016;93:075404. DOI: 10.1103/PhysRevB.93.075404
- [29] Kuang, Y. D., Lindsay, L., Shi, S. Q. & Zheng, G. P. Tensile strains give rise to strong size effects for thermal conductivities of silicene, germanene and stanene. *Nanoscale*, 2016;8:3760–3767. DOI: 10.1039/C5NR08231E
- [30] Rodin, A. S., Carvalho, A. & Castro Neto, A. H. Strain-induced gap modification in black phosphorus. *Phys. Rev. Lett.*, 2014;112:176801. DOI: 10.1103/PhysRevLett.112.176801
- [31] Qiao, J., Kong, X., Hu, Z.-X., Yang, F. & Ji, W. High-mobility transport anisotropy and linear dichroism in few-layer black phosphorus. *Nat. Commun.*, 2014;5(4475):4475. DOI: 10.1038/ncomms5475
- [32] Churchill, H. O. H. & Jarillo-Herrero, P. Two-dimensional crystals: Phosphorus joins the family. *Nat. Nanotech.*, 2014;9(5):330–331. DOI: 10.1038/nnano.2014.85
- [33] Liu, H. et al. Phosphorene: an unexplored 2D semiconductor with a high hole mobility. *ACS Nano*, 2014;8(4):4033–4041. DOI: 10.1021/nn501226z
- [34] Li, L. et al. Black phosphorus field-effect transistors. *Nat. Nanotech.*, 2014;9(5):372–377. DOI: 10.1038/nnano.2014.35
- [35] Fei, R. et al. Enhanced thermoelectric efficiency via orthogonal electrical and thermal conductances in phosphorene. *Nano Lett.*, 2014;14:6393–6399. DOI: 10.1021/nl502865s
- [36] Xia, F., Wang, H. & Jia, Y. Rediscovering black phosphorus as an anisotropic layered material for optoelectronics and electronics. *Nat. Commun.*, 2014;5(4458):4458. DOI: 10.1039/C4CC05752J

- [37] Low, T., Engel, M., Steiner, M. & Avouris, P. Origin of photoresponse in black phosphorus phototransistors. *Phys. Rev. B*, 2014;90:081408. DOI: 10.1103/PhysRevB.90.081408
- [38] Koenig, S. P., Doganov, R. A., Schmidt, H., Castro Neto, A. H. & Zyilmaz, B. Electric field effect in ultrathin black phosphorus. *Appl. Phys. Lett.*, 2014;104(10):103106. DOI: 10.1063/1.4868132
- [39] Tran, V., Soklaski, R., Liang, Y. & Yang, L. Layer-controlled band gap and anisotropic excitons in few-layer black phosphorus. *Phys. Rev. B*, 2014;89:235319. DOI: 10.1103/PhysRevB.89.235319
- [40] Wei, Q. & Peng, X. Superior mechanical flexibility of phosphorene and few-layer black phosphorus. *Appl. Phys. Lett.*, 2014;104(25):251915. DOI: 10.1063/1.4885215
- [41] Jiang, J.-W. & Park, H. S. Negative poisson's ratio in single-layer black phosphorus. *Nat. Commun.*, 2014;5(4727):4727. DOI: 10.1038/ncomms5727
- [42] Qin, G. et al. Hinge-like structure induced unusual properties of black phosphorus and new strategies to improve the thermoelectric performance. *Sci. Rep.*, 2014;4(6946):6946. DOI: 10.1039/C4CP04858J
- [43] Lv, H. Y., Lu, W. J., Shao, D. F. & Sun, Y. P. Enhanced thermoelectric performance of phosphorene by strain-induced band convergence. *Phys. Rev. B*, 2014;90:085433. DOI: 10.1103/PhysRevB.90.085433
- [44] Zhu, Z. & Tománek, D. Semiconducting layered blue phosphorus: A computational study. *Phys. Rev. Lett.*, 2014;112:176802. DOI: 10.1103/PhysRevLett.112.176802
- [45] Zhu, J. et al. Revealing the origins of 3d anisotropic thermal conductivities of black phosphorus. *Adv. Electron. Mater.*, 2016;1600040. DOI: 10.1002/aelm.201600040
- [46] Luo, Z. et al. Anisotropic in-plane thermal conductivity observed in few-layer black phosphorus. *Nat. Commun.*, 2015;6:9572. DOI: 10.1038/ncomms9572
- [47] Lee, S. et al. Anisotropic in-plane thermal conductivity of black phosphorus nanoribbons at temperatures higher than 100 K. *Nat. Commun.*, 2015;6:9573. DOI: 10.1038/ncomms9573
- [48] Jang, H., Wood, J. D., Ryder, C. R., Hersam, M. C. & Cahill, D. G. Anisotropic thermal conductivity of exfoliated black phosphorus. *Adv. Mater.*, 2015;27:8017–8022. DOI: 10.1002/adma.201503466
- [49] Liu, T.-H. & Chang, C.-C. Anisotropic thermal transport in phosphorene: effects of crystal orientation. *Nanoscale*, 2015;7:10648–10654. DOI: 10.1039/C5NR01821H
- [50] Hong, Y., Zhang, J., Huang, X. & Zeng, X. C. Thermal conductivity of a two-dimensional phosphorene sheet: a comparative study with graphene. *Nanoscale*, 2015;7:18716–18724. DOI: 10.1039/C5NR03577E



- [51] Xu, W., Zhu, L., Cai, Y., Zhang, G. & Li, B. Direction dependent thermal conductivity of monolayer phosphorene: parameterization of Stillinger-Weber potential and molecular dynamics study. *J. Appl. Phys.*, 2015;117:214308. DOI: 10.1063/1.4922118
- [52] Zhang, Y.-Y., Pei, Q.-X., Jiang, J.-W., Wei, N. & Zhang, Y.-W. Thermal conductivities of single- and multi-layer phosphorene: a molecular dynamics study. *Nanoscale*, 2016;8:483–491. DOI: 10.1039/C5NR05451F
- [53] Zhu, L., Zhang, G. & Li, B. Coexistence of size-dependent and size-independent thermal conductivities in phosphorene. *Phys. Rev. B*, 2014;90:214302. DOI: 10.1103/PhysRevB.90.214302
- [54] Jain, A. & McGaughey, A. J. H. Strongly anisotropic in-plane thermal transport in single-layer black phosphorene. *Sci. Rep.*, 2015;5(8501):8501. DOI: 10.1039/C5NR04366B
- [55] Qin, G. et al. Anisotropic intrinsic lattice thermal conductivity of phosphorene from first principles. *Phys. Chem. Chem. Phys.*, 2015;17:4854. DOI: 10.1039/C4CP04858J
- [56] Hu, Z.-X., Kong, X., Qiao, J., Normand, B. & Ji, W. Interlayer electronic hybridization leads to exceptional thickness-dependent vibrational properties in few-layer black phosphorus. *Nanoscale*, 2016;8:2740–2750. DOI: 10.1039/C5NR06293D
- [57] Bonini, N., Garg, J. & Marzari, N. Acoustic phonon lifetimes and thermal transport in free-standing and strained graphene. *Nano Lett.*, 2012;12:2673–2678. DOI: 10.1021/nl202694m
- [58] Fugallo, G. et al. Thermal conductivity of graphene and graphite: Collective excitations and mean free paths. *Nano Lett.*, 2014;14:6109–6114. DOI: 10.1021/nl502059f
- [59] Barbarino, G., Melis, C. & Colombo, L. Intrinsic thermal conductivity in monolayer graphene is ultimately upper limited: a direct estimation by atomistic simulations. *Phys. Rev. B*, 2015;91:035416. DOI: 10.1103/PhysRevB.91.035416
- [60] Bhowmick, S. & Shenoy, V. B. Effect of strain on the thermal conductivity of solids. *J. Chem. Phys.*, 2006;125:164513. DOI: 10.1063/1.2361287
- [61] Yan, J.-A., Gao, S.-P., Stein, R. & Coard, G. Tuning the electronic structure of silicene and germanene by biaxial strain and electric field. *Phys. Rev. B*, 2015;91:245403. DOI: 10.1103/PhysRevB.91.245403
- [62] Xu, G. L., Wu, M. S., Ouyang, C. Y. & B. Strain-induced semimetal-metal transition in silicene. *Europhys. Lett. (EPL)*, 2012;99:17010. DOI: 10.1186/1556-276X-9-521
- [63] Lian, C. & Ni, J. Strain induced phase transitions in silicene bilayers: a first principles and tight-binding study. *AIP Adv.*, 2013;3:052102. DOI: 10.1063/1.4804246
- [64] Pei, Q.-X., Zhang, Y.-W., Sha, Z.-D. & Shenoy, V. B. Tuning the thermal conductivity of silicene with tensile strain and isotopic doping: a molecular dynamics study. *J. Appl. Phys.*, 2013;114:033526. DOI: 10.1063/1.4815960

- [65] Baskes, M. I. Modified embedded-atom potentials for cubic materials and impurities. *Phys. Rev. B*, 1992;46:2727–2742. DOI: 10.1103/PhysRevB.46.2727
- [66] Tersoff, J. Modeling solid-state chemistry: interatomic potentials for multicomponent systems. *Phys. Rev. B*, 1989;39:5566–5568. DOI: 10.1103/PhysRevB.39.5566
- [67] Ong, Z.-Y., Cai, Y., Zhang, G. & Zhang, Y.-W. Strong thermal transport anisotropy and strain modulation in single-layer phosphorene. *J. Phys. Chem. C*, 2014;118:25272–25277. DOI: 10.1021/jp5079357
- [68] Zhang, X., Bao, H. & Hu, M. Bilateral substrate effect on the thermal conductivity of two-dimensional silicon. *Nanoscale*, 2015;7:6014–6022. DOI: 10.1039/C4NR06523A
- [69] Wang, Z., Feng, T. & Ruan, X. Thermal conductivity and spectral phonon properties of free-standing and supported silicene. *J. Appl. Phys.*, 2015;117(8):084317. DOI: 10.1063/1.4913600
- [70] Zhang, X., Gao, Y., Chen, Y. & Hu, M. Robustly engineering thermal conductivity of bilayer graphene by interlayer bonding. *Sci. Rep.*, 2016;6:22011. DOI: 10.1038/srep22011

